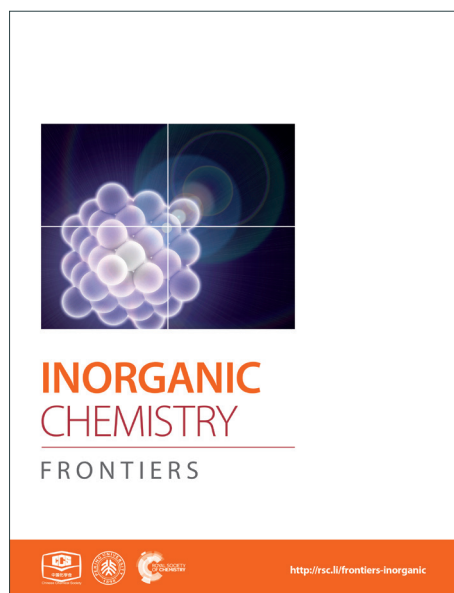
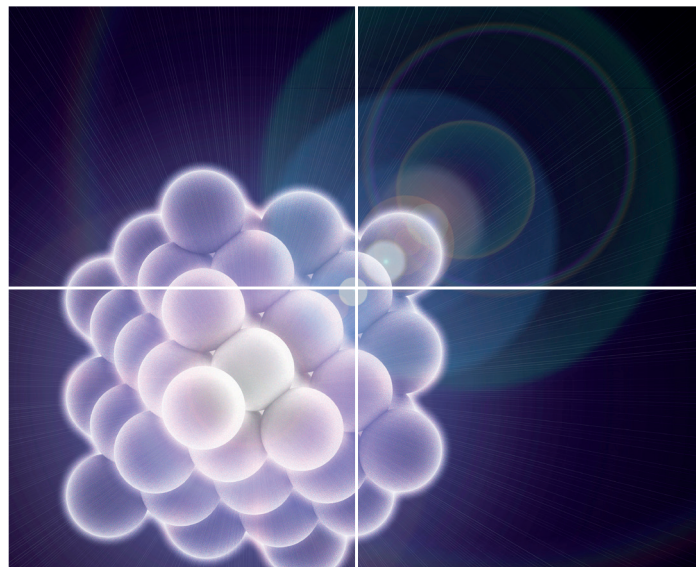


# INORGANIC CHEMISTRY

FRONTIERS

Accepted Manuscript



This is an *Accepted Manuscript*, which has been through the Royal Society of Chemistry peer review process and has been accepted for publication.

*Accepted Manuscripts* are published online shortly after acceptance, before technical editing, formatting and proof reading. Using this free service, authors can make their results available to the community, in citable form, before we publish the edited article. We will replace this *Accepted Manuscript* with the edited and formatted *Advance Article* as soon as it is available.

You can find more information about *Accepted Manuscripts* in the [Information for Authors](#).

Please note that technical editing may introduce minor changes to the text and/or graphics, which may alter content. The journal's standard [Terms & Conditions](#) and the [Ethical guidelines](#) still apply. In no event shall the Royal Society of Chemistry be held responsible for any errors or omissions in this *Accepted Manuscript* or any consequences arising from the use of any information it contains.

# Transesterification of dimethyl carbonate with phenol to diphenyl carbonate over hexagonal Mg(OH)<sub>2</sub> nanoflakes

Qiang Wang<sup>a,\*</sup>, Chunhong Li<sup>b</sup>, Ming Guo<sup>a</sup>, Shengjun Luo<sup>c</sup> and Changwen Hu<sup>d,\*</sup>

<sup>a</sup>Laboratory for Micro-sized Functional Materials & College of Elementary Education, Capital Normal University, Beijing, P R China. E-mail: qwchem@gmail.com; Fax: +86 10 68901751; Tel: +86 10 68902523

<sup>b</sup>National Laboratory for Superconductivity, Institute of Physics and Beijing National Laboratory for Condensed Matter Physics, Chinese Academy of Sciences, Beijing, P R China

<sup>c</sup>Qingdao Institute of Bioenergy and Bioprocess Technology, Chinese Academy of Sciences, Qingdao, P R China

<sup>d</sup>Key Laboratory of Cluster Science of Ministry of Education of China, The Institute for Chemical Physics and Department of Chemistry, Beijing Institute of Technology, Beijing, P R China. E-mail: cw hu@bit.edu.cn; Fax/ Tel: +86 10 68912631

## Abstract

Hexagonal Mg(OH)<sub>2</sub> nanoflakes were synthesized via a hydrothermal method in the presence of polyethylene glycol 20,000 (PEG-20,000). X-ray diffraction (XRD), field-emission scanning electron microscopy (FE-SEM) were applied to characterize the composition, morphologies and structure of the Mg(OH)<sub>2</sub> nanoflakes. Brunauer-Emmett-Teller (BET) analysis were performed to investigate the porous structure and surface area of the as-obtained nanoflakes. The transesterification of dimethyl carbonate (DMC) with phenol to produce diphenyl carbonate (DPC) was

carried out over the hexagonal  $\text{Mg}(\text{OH})_2$  nanoflakes. The evaluation results showed that the hexagonal  $\text{Mg}(\text{OH})_2$  nanoflakes had better activity and excellent selectivity to target products compared with many conventional ester exchange catalysts. Compared with other catalysts, such as  $\text{AlCl}_3$ ,  $\text{ZnCl}_2$ , and irregular  $\text{Mg}(\text{OH})_2$  synthesized via hydrothermal method without PEG-20,000, which all have been widely used as catalysts for this transesterification reaction,  $\text{Mg}(\text{OH})_2$  nanoflakes were more stable and showed a relatively high activity with a low catalyst amount. The transesterification reaction process was also analyzed with the classic thermodynamic theory, and when the reaction was carried out at 453 K, with a molar ratio of phenol to DMC of 2:1, a reaction time of 13 h, and a catalyst amount of 0.2% (molar ratio to phenol), the selectivity of the transesterification reaction reached 92.3%. Moreover, the deactivated hexagonal  $\text{Mg}(\text{OH})_2$  nanoflakes could be easily reactivated by calcination under vacuum, and the regenerated  $\text{Mg}(\text{OH})_2$  nanoflakes showed the catalytic activity almost as high as that of the fresh sample.

**Keywords:** catalytic behavior, hexagonal  $\text{Mg}(\text{OH})_2$  nanoflakes, transesterification, DPC, DMC

## Introduction

Transesterification is an important organic transformation and provides necessary synthons for a number of applications in organic processes.<sup>1-5</sup> The synthesis of aromatic carbonates from dimethyl carbonate (DMC) and phenols is one of the most important transesterification reactions. DMC is an important intermediate for organic synthesis because its molecular structure contains several functional groups, such as carbonyl, methyl and methoxy. Moreover, it is nontoxic for human health and environment. Meanwhile, aromatic carbonates, especially diphenyl carbonate (DPC), are precursors for the production of aromatic polycarbonates by the melt

polymerization process which is now the highlight in the polycarbonate industry.<sup>6-31</sup> DPC is widely used as a starting material for phosgene-free polycarbonates production by interfacial polycondensation. Because of the increasing demand for a safe and environmental friendly process of DPC synthesis, several non-phosgene methods have been developed.<sup>1-31</sup> Among them, the most suitable method route is the oxidative carbonylation of phenol, which is a single-step process with water as the sole byproduct.<sup>1</sup> This route is a two-step process, which involving the transesterification of DMC and phenol to methyl phenyl carbonate (MPC) (Eq. 1) and the further transesterification of MPC and phenol (Eq. 2) or disproportion of MPC to DPC (Eq. 3) and the O-methylation reaction (Eq. 4) shown in Scheme 1.

The synthesis of DPC by transesterification of DMC with phenol is usually catalyzed by organometallic compounds containing titanium, aluminium, tin, and conventional Lewis acid catalysts such as aluminium chloride and zinc chloride.<sup>1-29</sup> The homogeneous catalysts such as conventional Lewis acids,<sup>16-19</sup> titanium esters,<sup>18</sup> tin compounds,<sup>19</sup> titanocene dichloride ( $\text{Cp}_2\text{TiCl}_2$ ),<sup>20</sup> samarium halogen,<sup>7,21</sup> and mesoporous MCM-41<sup>22</sup> have been used as effective catalysts for the transesterification of DMC with phenol. But the reuse of these catalysts is very difficult because it is not easy to separate and recover these catalysts. Furthermore, the titanium and tin compounds are so poisonous and harmful to the environment. Consequently, many heterogeneous catalysts such as  $\text{MoO}_3/\text{SiO}_2$ ,<sup>23</sup>  $\text{TiO}_2/\text{SiO}_2$ ,<sup>24</sup> Mg-Al-hydrotalcite,<sup>25</sup>  $\text{PbO}/\text{MgO}$ ,<sup>26,27</sup>  $\text{NNC}$ ,<sup>28</sup> and  $\text{MCN-TiO}_2$ <sup>29</sup> were investigated for this reaction. Disappointedly, these catalysts not only produce the byproduct anisole more or less due to their alkalescency, but they also terminate the reaction in the first step making MPC the main product, as shown in Eq. 1. Also, Tundo et al.<sup>30</sup> reported that the equilibrium constant for Eq. 1 was  $3 \times 10^{-4}$  at 453 K. This indicates that the

transesterification reactions are thermodynamically unfavorable, while the O-methylation Eq. 4 is thermodynamically favorable due to the production of gaseous  $\text{CO}_2$ . To overcome the thermodynamic limitation of the transesterification reactions, many processes have been proposed.<sup>1-31</sup> Therefore, it is desirable to find more efficient, innocuous and cheap catalysts for transesterification of DMC with phenol in the application of commercial production.

Here, hexagonal  $\text{Mg}(\text{OH})_2$  nanoflakes with a thickness of about ~10 nm and a lateral size of about ~100 nm in the presence of PEG-20,000 were synthesized via hydrothermal process. More importantly, the hexagonal  $\text{Mg}(\text{OH})_2$  nanoflakes showed excellent catalytic activities for the transesterification of DMC and phenol. Although the synthesis of  $\text{Mg}(\text{OH})_2$  has been studied by many researchers,<sup>32</sup> to the best of our knowledge, there is no report on discussing the catalytic behavior of  $\text{Mg}(\text{OH})_2$  nanostructures yet.

## Experimental

### Materials

Dimethyl carbonate and phenol were obtained from Alfa Aesar. Magnesium nitrate hexahydrate(AR), sodium hydroxide (AR), Polyethylene glycol ( $M_w \approx 20,000$ ), ethanol (AR), and Acetone (AR) were purchased from Beijing Chemical Reagent Company, China. All of the materials and reagents were used directly without further purification. Distilled water was purified using a Milli-Q system (Millipore, Billerica, MA).

### Preparation of hexagonal $\text{Mg}(\text{OH})_2$ nanoflakes

The hexagonal  $\text{Mg}(\text{OH})_2$  nanoflakes were prepared by the classical methods. In a typical synthesis, 0.2 g of hydrated magnesium nitrate ( $\text{Mg}(\text{NO}_3)_2 \cdot 6\text{H}_2\text{O}$ ) and 0.1 g of PEG-20,000 were each dissolved in 30 mL of deionized water. Then the aqueous

solution of PEG-20,000 was added dropwise to the aqueous  $\text{Mg}^{2+}$  solution under constant stirring. The mixture was stirred until a clear and homogeneous solution formed, and 1 mL of  $1.0 \text{ mol} \cdot \text{L}^{-1}$  NaOH solution was added to the homogeneous solution. Then the new formed suspension was transferred to an 80 mL Teflon-lined autoclave, which was sealed and maintained at 433 K for 12 h. After the autoclave was cooled to room temperature, the resulting white precipitate was collected, washed several times with distilled water and absolute ethanol and dried at 373 K for 4 h.

### **Characterization of $\text{Mg}(\text{OH})_2$ samples**

The composition, morphologies and structures of  $\text{Mg}(\text{OH})_2$  samples were characterized by X-ray powder diffraction (XRD, Shimadzu XRD-6000, Cu  $\text{K}\alpha$  radiation ( $\lambda = 1.54 \text{ \AA}$ )), field-emission scanning electron microscopy (FE-SEM, Hitachi S-4800) with an accelerating voltage of 10 kV. The specific surface structure of the  $\text{Mg}(\text{OH})_2$  samples were determined on a constant volume adsorption apparatus (CHEMBET-3000) by the  $\text{N}_2$ -BET method at liquid nitrogen temperature. And the catalytic properties of the  $\text{Mg}(\text{OH})_2$  samples were examined on-line by gas-chromatogram (GC) (Shimadzu GC-2014). The surface composition and structure of catalyst were studied by X-ray photoelectron spectroscopy (XPS, ThermoFisher Scientific, USA, ESCALAB 250) with Al  $\text{K}\alpha$  radiation (1487 eV) at a power of 300 W under a vacuum of  $1.0 \times 10^{-5}$  Pa. Data were analyzed by use of XPSpeak 41 software.

### **Typical procedure for transesterification**

The typical procedure for the transesterification of DMC and phenol is as follows: All transesterification reactions were carried out in a 100 mL four-necked round-bottomed flask equipped with a magnetic stirring bar, a nitrogen inlet, a precise plunger pump for DMC instillation, and a Vigreux fractionating column connected to

a liquid dividing head. Typical conditions and procedures were as follows: phenol (0.2 mol) and the catalyst (0.5 mmol) were charged into the reactor under nitrogen atmosphere, and the temperature was gradually raised to and kept at 453 K. Then DMC was added drop-wise into the reactor at a flow rate of 0.05 ml/min using the precise plunger pump. The reaction mixture was under refluxing condition during the period of reaction. The occurrence of reaction was indicated by attainment of temperature of about 333 K at the top of the column. During the reaction, this distillation was analyzed by GC one time per hour.<sup>1-7</sup> The reaction mixture was identified by the absolute retention time and quantified with ethyl benzoate as internal standard method. After the reaction, the mixture was cooled to room temperature, the catalyst was filtrated and washed. The deactivated hexagonal Mg(OH)<sub>2</sub> nanoflakes could be easily reactivated by calcination at 573 K under vacuum, and the regenerated Mg(OH)<sub>2</sub> nanoflakes showed the catalytic activity almost as high as that of the fresh sample.

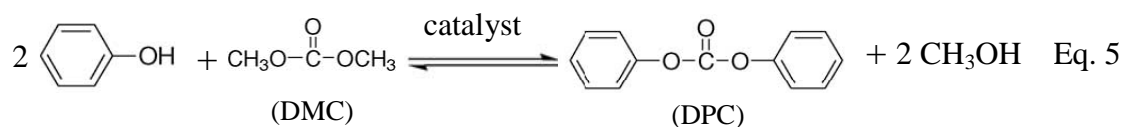
## Results and discussion

The composition and purity of the as-synthesized Mg(OH)<sub>2</sub> flakes were examined by X-ray diffraction (Fig. 1). All of the diffraction peaks in Fig. 1a can be indexed as the pure hexagonal phase of Mg(OH)<sub>2</sub> [space group:  $P\bar{3}m1[164]$ ] with lattice constants of  $a = b = 3.144 \text{ \AA}$  and  $c = 4.777 \text{ \AA}$  (JCPDS card No. 44-1482) and angle constants of  $\alpha = \beta = 90^\circ$  and  $\gamma = 120^\circ$ . As shown in Fig. 2, the hexagonal Mg(OH)<sub>2</sub> nanoflakes have a layered structure. Fig. 1b shows the amorphous structure of magnesium hydroxide synthesized without the presence of PEG-20,000.

Representative field-emission scanning electron micrographs (FE-SEM) of the as-synthesized Mg(OH)<sub>2</sub> samples are shown in Fig. 3. An overview image (Fig. 3a) discloses that the sample entirely consists of flake-shaped particles without the

presence of other morphological structures. The higher magnification FE-SEM image inserted in Fig. 3a clearly reveals that each particle consists almost entirely of well-defined hexagonal nanoflakes with a thickness of ~10 nm and a lateral dimension of ~100 nm. The overall hexagonal morphology of these Mg(OH)<sub>2</sub> particles is consistent with the hexagonal crystallographic characteristics of brucite. The amorphous structures of magnesium hydroxide synthesized without the presence of PEG-20,000 are showed in Fig. 3b, which are disorganized morphologies.

The stoichiometric equation for the transesterification of DMC with phenol is as follows:



The chemical equilibrium and the reaction kinetics were probed in the expected operating range of the transesterification process, during which the temperature was varied between 298 K and 523 K. On the basis of references<sup>25,33-36</sup>, the thermodynamic data for Eqs. 5 and 1 were calculated and shown in Table 1 and Table 2. According to Table 1, the transesterification Eq. 5 is endothermic at temperatures below 453 K, and the equilibrium constant ( $K_{\text{eq}}^{\ominus}$ ) increases with the increase of temperature. When the temperature is above 453 K, phenol is vaporized, and Eq. 5 becomes exothermic. Between 423 K and 523 K,  $K_{\text{eq}}^{\ominus}$  remains almost the same. Thus, the suitable temperature for Eq. 5 should be 423 K~453 K. Because of the Eq. 1 is endothermic, a higher temperature is preferable for this reaction (see Table 2). The thermodynamic data in Tables 1 and 2 show that the transesterification of DMC with phenol is thermodynamically unfavorable even at 523 K, while the reaction of O-methylation of DMC with phenol is thermodynamically favorable at room temperature. Thus, to choose a suitable temperature and to design an efficient reaction

process are the keys to increasing not only the yields of DPC and MPC but also the selectivities to them. According to Table 1 and Table 2, the temperature of the transesterification of DMC with phenol was selected as 453 K, and the standard enthalpy for the exothermic reaction of have been determined which was subsequently integrated into the energy balances of the transesterification process model accounting for the heat supplied by the chemical reaction.<sup>36</sup>

The catalytic properties of hexagonal  $\text{Mg}(\text{OH})_2$  nanoflakes for the transesterification of DMC with phenol were also investigated (Fig. 4a). For comparison, the catalytic behavior of irregular  $\text{Mg}(\text{OH})_2$  flakes (Fig. 4b),  $\text{AlCl}_3$  (Fig. 4c) and  $\text{ZnCl}_2$  (Fig. 4d) for the transesterification were also provided. The yield of ester, selectivities to MPC and DPC were shown in Fig. 4, and the detailed results were summarized in Table 3. The synthesis of DPC is usually performed in two steps, as shown in Eqs. 1, 2, 3 and 4.

In the first step, phenol is converted into methyl phenyl carbonate (MPC), and in the second step, MPC is converted into DPC by the reaction with phenol. MPC is the intermediate product during the transesterification, which is also a valuable industrial, and in some cases, the anisole (AN) may be produced as a byproduct during the second step (Eq. 4).

As shown in Fig. 4 and Table 3, the transesterification selectivity for hexagonal  $\text{Mg}(\text{OH})_2$  nanoflakes is 92.3%, which is the highest of the four catalysts, while the selectivities for  $\text{AlCl}_3$ ,  $\text{ZnCl}_2$ , and irregular  $\text{Mg}(\text{OH})_2$  flakes range from 70% to 80%. The selectivities to DPC for  $\text{Mg}(\text{OH})_2$  hexagonal nanoflakes' and irregular  $\text{Mg}(\text{OH})_2$  flakes' selectivities toward DPC are 32.6% and 26.1%, but the selectivities toward MPC are 59.7% and 49.6%, respectively. Table 3 is showing an overview of the selectivities for DPC and MPC for the various catalysts tested. When compared, the

hexagonal  $\text{Mg}(\text{OH})_2$  nanoflakes have the highest selectivity towards MPC while  $\text{ZnCl}_2$  has the highest selectivity toward DPC. It is also worth noting that  $\text{AlCl}_3$  had the highest yield of the byproduct anisole.

It is known that the activities and selectivities of the various catalysts may be influenced by the acidity or alkalinity of the catalysts.<sup>1-27</sup>  $\text{AlCl}_3$  and  $\text{ZnCl}_2$  are typical Lewis acid catalysts, which are known to accelerate Eq. 2 and 3 in Scheme 1, while the hexagonal  $\text{Mg}(\text{OH})_2$  nanoflakes and irregular  $\text{Mg}(\text{OH})_2$  flakes are alkaline compounds, which are known to speed up Eq. 1 in Scheme 1. It is generally accepted that the more alkaline a catalyst is, the higher the yield and selectivity of the relevant products will be. The appropriate alkalescence is also an important factor for transesterification activity. As shown above, hexagonal  $\text{Mg}(\text{OH})_2$  nanoflakes have the highest overall transesterification selectivity, which may be due to its high alkalinity on the surface of the nanoflakes. In addition, in the above catalytic process, the hexagonal  $\text{Mg}(\text{OH})_2$  nanoflakes are not dissolved or decomposed during the transesterification and once collected, 97.8% of the nanoflakes can be recycled. The transesterification catalyzed by hexagonal  $\text{Mg}(\text{OH})_2$  nanoflakes is also an unpolluted process. Hence, hexagonal  $\text{Mg}(\text{OH})_2$  nanoflakes are more suitable for the transesterification of DMC with phenol when compared with  $\text{AlCl}_3$ ,  $\text{ZnCl}_2$  and irregular  $\text{Mg}(\text{OH})_2$  flakes.

One of the important criteria for heterogeneous catalysis is the reusability. The possibility and extent of catalyst deactivation was investigated by employing the recycled catalyst sample washed by DMC and dried at 373 K in a number of reaction cycles, which is given in Table 4. Table 4 showed that the hexagonal  $\text{Mg}(\text{OH})_2$  nanoflakes exhibited a decline in activity with reuse. According to the total yield of the esters (MPC and DPC), the activity of the catalyst used once reduced only 5%,

from 23.9 to 22.7%. When it was used for the fifth time, the activity of the catalyst reduced about a half, from 23.9 to 13.1%. It was interesting that the total selectivity of MPC and DPC increased slightly with the decrease of total yield of the esters, which might suggest some structure sensitivity in terms of transesterification selectivity. Moreover, the hexagonal  $\text{Mg}(\text{OH})_2$  nanoflakes used fifth was regenerated by calcination at 573 K under vacuum, the result is also shown in Table 4. The total yield of the esters reached to 21.7%, which was a little lower than that of the fresh hexagonal  $\text{Mg}(\text{OH})_2$  nanoflakes. It presented that the catalytic activity could almost be recovered by calcination of the used catalyst.

Based on above experimental results, the transesterification mechanism catalyzed by the hexagonal  $\text{Mg}(\text{OH})_2$  nanoflakes was suggested as the following procedure (Fig. 5).<sup>1,20</sup> At first, the  $\text{Mg}^{2+}$  was exposed(I) in the crystal structure of  $\text{Mg}(\text{OH})_2$ . According to the charge distribution and the theory of coordination chemistry, the weak interaction between the O atom of carbonyl in DMC and the  $\text{Mg}^{2+}$  would make DMC and  $\text{Mg}(\text{OH})_2$  to form  $\text{Mg}(\text{OH})_2(\text{DMC})(\text{II})$ . The transesterification of DMC and phenol belongs to a reaction of soft base binding to hard acid, the active center  $\text{sp}^2$ -hybridized carbonyl carbon in DMC was regarded as a hard acid center. The carbonyl carbon in DMC was affected by the carbonyl oxygen with larger electronegativity, so that electrons would tend to carbonyl oxygen resulting in the electron cloud density of carbon atom decreasing and the carbonyl carbon positively charged. So the carbonyl carbon had a strong electrophilic activity and was the electrophilic center. Meanwhile, the negatively charged oxygen atoms of  $\text{C}_6\text{H}_5\text{O}^-$  contain lone electron pairs and the ability to attract electrons is stronger than the carbon atoms on the benzene ring, the oxygen atoms prone to nucleophilic reactions. As a result, the carbonyl carbon in DMC should be attacked more easily by  $\text{C}_6\text{H}_5\text{O}^-$  to

produce intermediate (III). After the rearrangement, it might either demethoxylate to give  $\text{Mg}(\text{OH})_2(\text{MPC})(\text{IV})$  or dephenoxyate to yield  $\text{Mg}(\text{OH})_2(\text{DMC})(\text{II})$ . The DMC or MPC can leave from the intermediate (II) or (IV), respectively, agreed to Eq. 1 in Scheme 1. The transformation of  $\text{Mg}(\text{OH})_2(\text{MPC})(\text{IV})$  to intermediate (V) is similar to the procedure of (II)–(III). The intermediate (V) may also demethoxylate to produce  $\text{Mg}(\text{OH})_2(\text{DPC})(\text{VI})$  or dephenoxyate to return  $\text{Mg}(\text{OH})_2(\text{DMC})(\text{II})$ . The MPC or DPC also leaves from the (IV) or (VI), respectively, as showed in Eq. 2. The intermediates (II, IV and VI) can return back to (I) with the leaving of DMC, MPC or DPC, respectively, resulting in the completed catalytic cycle. This mechanism explains the high selectivity of ester in this transesterification.

In addition, the higher activity of the hexagonal  $\text{Mg}(\text{OH})_2$  nanoflakes when compared to the irregular  $\text{Mg}(\text{OH})_2$  flakes can be ascribed to their relatively higher surface area. The isotherms of nitrogen adsorption and desorption at 77 K for hexagonal  $\text{Mg}(\text{OH})_2$  nanoflakes and irregular  $\text{Mg}(\text{OH})_2$  flakes are plotted in Fig. 6a and Fig. 6b, respectively. The isotherms for the hexagonal  $\text{Mg}(\text{OH})_2$  nanoflakes and irregular  $\text{Mg}(\text{OH})_2$  flakes are characteristic of a type IV isotherm with a type  $\text{H}_3$  hysteresis loop. Also, the pore volume and pore diameter distribution plots of hexagonal  $\text{Mg}(\text{OH})_2$  nanoflakes and irregular  $\text{Mg}(\text{OH})_2$  flakes were inserted in Fig.6, which indicated the presence of mesopores in the size range 2-110 nm. The pore size distribution testing presented that the average pore size of hexagonal  $\text{Mg}(\text{OH})_2$  nanoflakes and irregular  $\text{Mg}(\text{OH})_2$  flakes were 10.39 nm and 17.67 nm, respectively. Therefore, the number of holes per unit area of the hexagonal  $\text{Mg}(\text{OH})_2$  nanoflakes was more than the irregular  $\text{Mg}(\text{OH})_2$  flakes. On the basis of the isotherms, it is possible to calculate the values of the BET surface area ( $S_{\text{BET}}$ );  $S_{\text{BET}}$  values of the hexagonal  $\text{Mg}(\text{OH})_2$  nanoflakes and irregular  $\text{Mg}(\text{OH})_2$  flakes are 68.87 and 42.48

$\text{m}^2/\text{g}$ , respectively. The  $S_{\text{BET}}$  values of the hexagonal  $\text{Mg}(\text{OH})_2$  nanoflakes are larger than that of irregular  $\text{Mg}(\text{OH})_2$  flakes, because the hexagonal  $\text{Mg}(\text{OH})_2$  nanoflakes are smaller than the irregular  $\text{Mg}(\text{OH})_2$  flakes and the latter easily tend to agglomerate (Fig. 3). On the basis of the catalytic tests and the surface area measurements shown in Fig. 4, Table 3 and Fig. 6, it can be concluded that between these two samples, the sample with the largest surface area may possess the highest amount of active centers which then offers the highest selectivity towards DPC. So the hexagonal  $\text{Mg}(\text{OH})_2$  nanoflakes with a high surface area and suitable pores are more effective as a catalyst than the irregular counterpart in the transesterification.

XPS results for the hexagonal  $\text{Mg}(\text{OH})_2$  nanoflakes and irregular  $\text{Mg}(\text{OH})_2$  flakes were shown in Fig. 7. XPS analysis was used to determine the elements of the surface of the samples.<sup>37-39</sup> Fig. 7a showed sharp peaks with a binding energy of 56.8 eV, 530.4 eV and 1309.6 eV. Taking the known binding energy of  $\text{Mg}(\text{OH})_2$  into consideration. The relative content of  $\text{Mg}(+2, 2\text{p})$  and  $\text{Mg}(+2, 1\text{s})$  were 27.13 and 25.13%, respectively. Fig. 7b also showed the similar peaks with Fig. 7a, the relative content of  $\text{Mg}(+2, 2\text{p})$  and  $\text{Mg}(+2, 1\text{s})$  were about 18.44 and 10.40%, respectively. The high-resolution  $\text{O}(1\text{s})$  XPS spectra of the film surfaces revealed one component at a binding energy of 530.4 eV associated with the  $\text{OH}^-$ . According to Fig. 7, the content of the  $\text{Mg}(+2)$  ions on the surface of the hexagonal nanoflakes was higher than that of the irregular  $\text{Mg}(\text{OH})_2$  flakes, which was consistent with the BET analysis and the appropriate catalytic behavior of themselves. Also, this further provided a basis for the transesterification mechanism (shown in Fig.5) that  $\text{Mg}^{2+}$  played a key role in the process of the formation of intermediate products, such as  $\text{Mg}(\text{OH})_2(\text{DMC})(\text{II})$ ,  $\text{Mg}(\text{OH})_2(\text{MPC})(\text{IV})$  and  $\text{Mg}(\text{OH})_2(\text{DPC})(\text{VI})$ .

## Conclusions

The hexagonal  $\text{Mg}(\text{OH})_2$  nanoflakes were successfully synthesized in large quantities via a hydrothermal method in the presence of PEG-20,000. The composition, morphology and structure of the hexagonal  $\text{Mg}(\text{OH})_2$  nanoflakes were characterized by XRD, FE-SEM, and BET. The hexagonal  $\text{Mg}(\text{OH})_2$  nanoflakes were an active catalyst for the synthesis of DPC from the transesterification of DMC with phenol. The transesterification selectivity for hexagonal  $\text{Mg}(\text{OH})_2$  nanoflakes is 92.3%. The selectivities to DPC for  $\text{Mg}(\text{OH})_2$  hexagonal nanoflakes' and irregular  $\text{Mg}(\text{OH})_2$  flakes' selectivities toward DPC are 32.6% and 26.1%, but the selectivities toward MPC are 59.7% and 49.6%, respectively. In general, the hexagonal  $\text{Mg}(\text{OH})_2$  nanoflakes were found to be one novel and efficient heterogeneous catalyst for the synthesis of DPC by transesterification of DMC with phenol. Moreover, the deactivated hexagonal  $\text{Mg}(\text{OH})_2$  nanoflakes could be easily reactivated by calcination under vacuum and can be reused.

### Acknowledgements

This work was supported by the Natural Science Foundation of China (NSFC, Nos. 21471103, 21471100, 51002180, 21001074, 20731002, 20871016, 10876002, 91022006 and 20973023), the 111 Project (B07012), the Fundamental Research Funds for the Central Universities (2013NT13), the Project of Excellent Talents of Beijing (203135407707), and the Scientific Research Base Development Program of the Beijing Municipal Commission of Education.

### References

- 1 S. J. Luo, Y. N. Chi, L. N. Sun, Q. Wang and C. W. Hu, *Catalysis Communications*, 2008, 9, 2560.
- 2 P. Braustein, M. Lakkis and D. Matt, *J. Mol. Catal.*, 1987, 42, 353.
- 3 A.G. Shaikh and S. Sivaram, *Ind. Eng. Chem. Res.*, 1992, 31, 1167.

- 4 H. Y. Niu, J. Yao, Y. Wang and G. Y. Wang, *J. Molecular Catalysis A: Chemical*, 2005, 235, 240.
- 5 Q. Wang, S. J. Luo, M. H. Cao and C. W. Hu, *J. Beijing Institute of Technology*, 2008, 17, 87.
- 6 Q. Wang, K. L. Wang, X. L. Wu, S. J. Luo and C. W. Hu, *Chem. Res. Chinese U.*, 2007, 23, 641.
- 7 F. M. Mei, G. X. Li, J. Nie and H. B. Xu, *J. Molecular Catalysis A: Chemical*, 2002, 184, 465.
- 8 Y. Watanabe and T. Tatsumi, *Micro. Meso. Mater.*, 1998, 22, 399.
- 9 C. H. Yang, W. B. Li, Y. Q. Liu, Y. S. Tan and Y. Z. Han, *J. Fuel Chem. Tech.*, 2002, 30, 551.
- 10 Z. H. Li, Z. F. Qin and J. G. Wang, *Petrochemical Technology*, 2006, 35, 528.
- 11 F. Y. Pan, S. P. Wang, X. B. Ma, Z. H. Li and G.H. Xu, *Chemical Industry & Engineering*, 2004, 21, 174.
- 12 Y. Liu, S. P. Wang and X. B. Ma, *Ind. Eng. Chem. Res.*, 2007, 46, 1045.
- 13 D. X. Yin, Z. H. Li, T. L. Xiang, B. W. Wang, X. B. Ma and G. H. Xu, *Natural Gas Chem. Industry*, 2004, 29, 20.
- 14 Y. Z. Li and S. J. Kim, *J. Phys. Chem. B.*, 2005, 109, 12309.
- 15 A. Prakash, A. V. McCormick and M. R. Zachariah, *Chem. Mater.*, 2004, 16, 1466.
- 16 Z. Li and Z. Qin, *J. Mol. Catal. A: Chem.*, 2007, 264, 255.
- 17 K. M. Deshmukh, Z. S. Qureshi, K. P. Dhake and B. M. Catal. Commun., 2010, 12, 207.
- 18 H. Lee, S. J. Kima, B. S. Ahna and W. K. Lee, *Catal. Today*, 2003, 87, 139.
- 19 A. Vimont, A. Travert, C. Binet, C. Pichon, P. Mialane, F. S cheresse and J. C.

- Lavalley, *J. Catal.*, 2006, 241, 221.
- 20 H. Y. Niu, J. Yao, Y. Wang and G. Y. Wang, *Catal. Commun.*, 2007, 8, 355.
- 21 H. Y. Niu, H. M. Guo, J. Yao, Y. Wang and G. Y. Wang, *J. Mol. Catal. A: Chem.*, 2006, 259, 292.
- 22 Y. Liu, G. M. Zhao, G. Liu, S. J. Wu, G. H. Chen, W. X. Zhang, H. Y. Sun and M. J. Jia, *Catal. Commun.*, 2008, 9, 2022.
- 23 Z. H. Fu and Y. Ono, *J. Mol. Catal. A: Chem.*, 1997, 118, 293.
- 24 R. Z. Tang, T. Chen, Y. Chen, Y. Z. Zhang, G. Y. Wang, *Chinese J. Catalysis*, 2014, 35, 457.
- 25 F. M. Mei, Z. Pei and G. X. Li, *Organic Process Research & Development*, 2004, 8, 372.
- 26 W. Q. Zhou, X. Q. Zhao, Y. J. Wang and J. Y. Zhang, *Appl. Catal. A: Gen.*, 2004, 260, 19.
- 27 Z. H. Li, Y. J. Wang, X. S. Ding, X. Q. Zhao, *J. Natural Gas Chem.*, 2009, 18, 104.
- 28 X. L. Yuan, M. Zhang, X. D. Chen, N. H. An, G. Liu, Y. Liu, W. X. Zhang, W. F. Yan, M. J. Jia, *Applied Catalysis A: General*, 2012, 439–440, 149.
- 29 X. Zhou, X. Ge, R. Z. Tang, T. Chen, G. Y. Wang, *Chinese J. Catalysis*, 2014, 35, 481.
- 30 P. Tundo, F. Trotta, G. Moraglio and F. Ligorati, *Ind. Eng. Chem. Res.*, 1988, 27, 1565-1571.
- 31 Y. Watanabe and T. Tatsumi, *Micro Meso Mater.*, 1998, 22, 399.
- 32 G. W. Beall, E. M. Duraia, F. El-Tantawy, F. Al-Hazmi and A. A. Al-Ghamdi, *Powder Technol.*, 2013, 234, 26.
- 33 G. C. Sinke, D. L. Hildenbrand, R. A. McDonald, W. R. Kramer and D. R. Stull, *J.*

- Phys. Chem.*, 1958, 62, 1461.
- 34 W. V. Steele, R. D. Chirico, S. E. Knipmeyer and A. Nguyen, *J. Chem. Eng. Data*, 1997, 42, 1008.
- 35 W. V. Steele, R. D. Chirico, S. E. Knipmeyer, A. Nguyen and N. K. Smith, *J. Chem. Eng. Data*, 1997, 42, 1037.
- 36 J. Holtbruegge, S. Heile, P. Lutze, A. Górak, *Chem. Eng. J.*, 2013, 234, 448.
- 37 D. S. Tong, J. Yao, Y. Wang, H. Y. Niu and G. Y. Wang, *J. Mol. Catal. A: Chem.*, 2007, 268, 120.
- 38 F. Z. Zhang, H. Zhang and Z. X. Su, *Appl. Surf. Sci.*, 2007, 253, 7393.
- 39 T. Ishizaki, R. Kudo, T. Omi, K. Teshima, T. Sonoda, I. Shigematsu, M. Sakamoto, *Electrochimica Acta*, 2012, 62, 19.

Captions of Figures, Tables and Scheme

**Fig. 1** XRD patterns of hexagonal  $\text{Mg}(\text{OH})_2$  nanoflakes (a) and irregular  $\text{Mg}(\text{OH})_2$  flakes (b).

**Fig. 2** Crystal structure of hexagonal  $\text{Mg}(\text{OH})_2$ .

**Fig. 3** FE-SEM images of hexagonal  $\text{Mg}(\text{OH})_2$  nanoflakes (a) and irregular  $\text{Mg}(\text{OH})_2$  flakes (b).

**Fig. 4** Catalytic activity of hexagonal  $\text{Mg}(\text{OH})_2$  nanoflakes (a), irregular  $\text{Mg}(\text{OH})_2$  flakes (b),  $\text{AlCl}_3$  (c) and  $\text{ZnCl}_2$  (d).

**Fig. 5** Plausible mechanism over hexagonal  $\text{Mg}(\text{OH})_2$  nanoflakes.

**Fig. 6**  $S_{\text{BET}}$  values of hexagonal  $\text{Mg}(\text{OH})_2$  nanoflakes (a) and irregular  $\text{Mg}(\text{OH})_2$  flakes (b).

**Fig. 7** XPS spectra for hexagonal  $\text{Mg}(\text{OH})_2$  nanoflakes (a) and irregular  $\text{Mg}(\text{OH})_2$  flakes (b).

**Table 1** Thermodynamic data in the transesterification of DMC with phenol at atmospheric pressure.

**Table 2** Thermodynamic data in the O-methylation of DMC with phenol at atmospheric pressure.

**Table 3** Transesterification of DMC with phenol catalyzed by hexagonal  $\text{Mg}(\text{OH})_2$  nanoflakes, irregular  $\text{Mg}(\text{OH})_2$  flakes,  $\text{AlCl}_3$  and  $\text{ZnCl}_2$ .

**Table 4** Numbers of catalyst reuse<sup>a</sup>.

**Scheme 1** Transesterification of DMC with phenol to DPC catalyzed by different catalysts.

Fig. 1

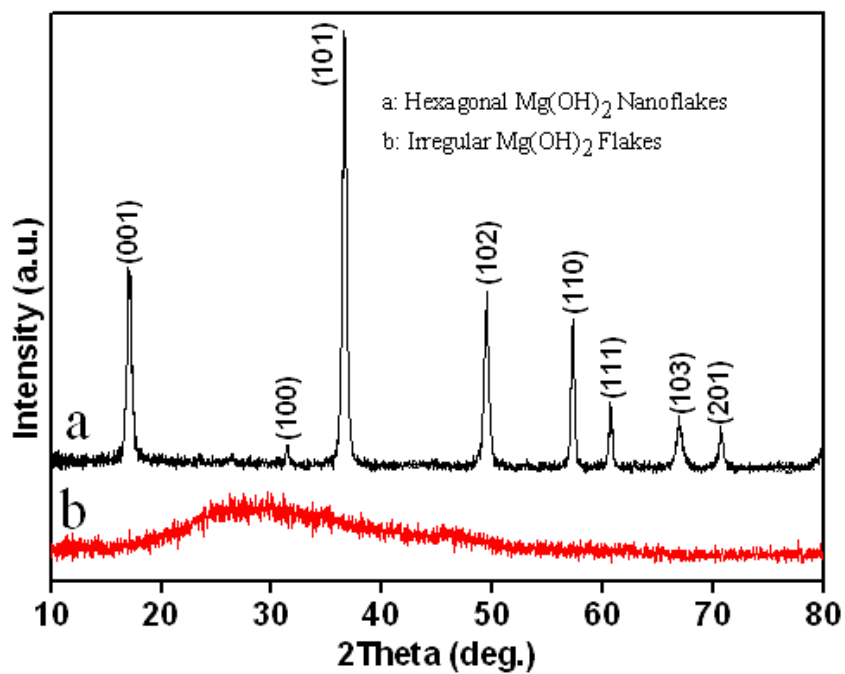


Fig. 2

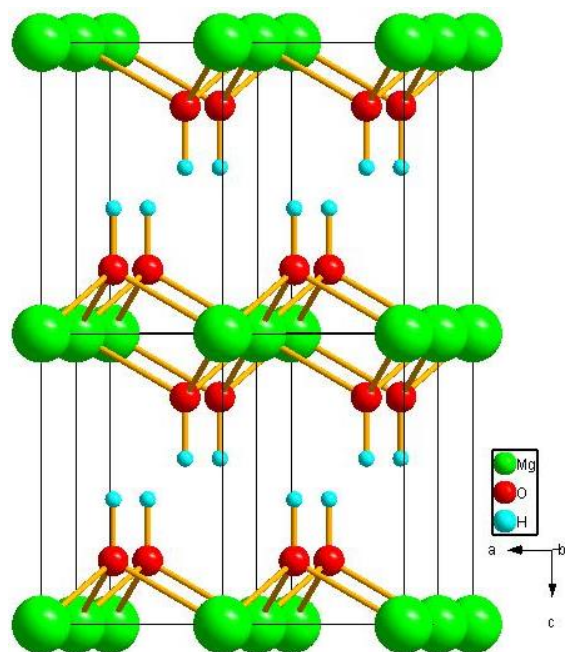


Fig. 3

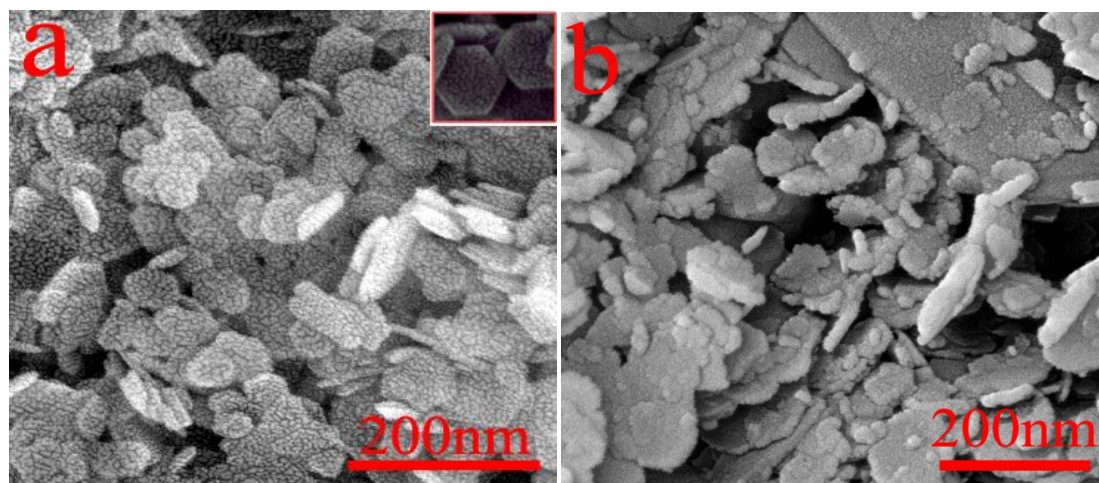


Fig. 4

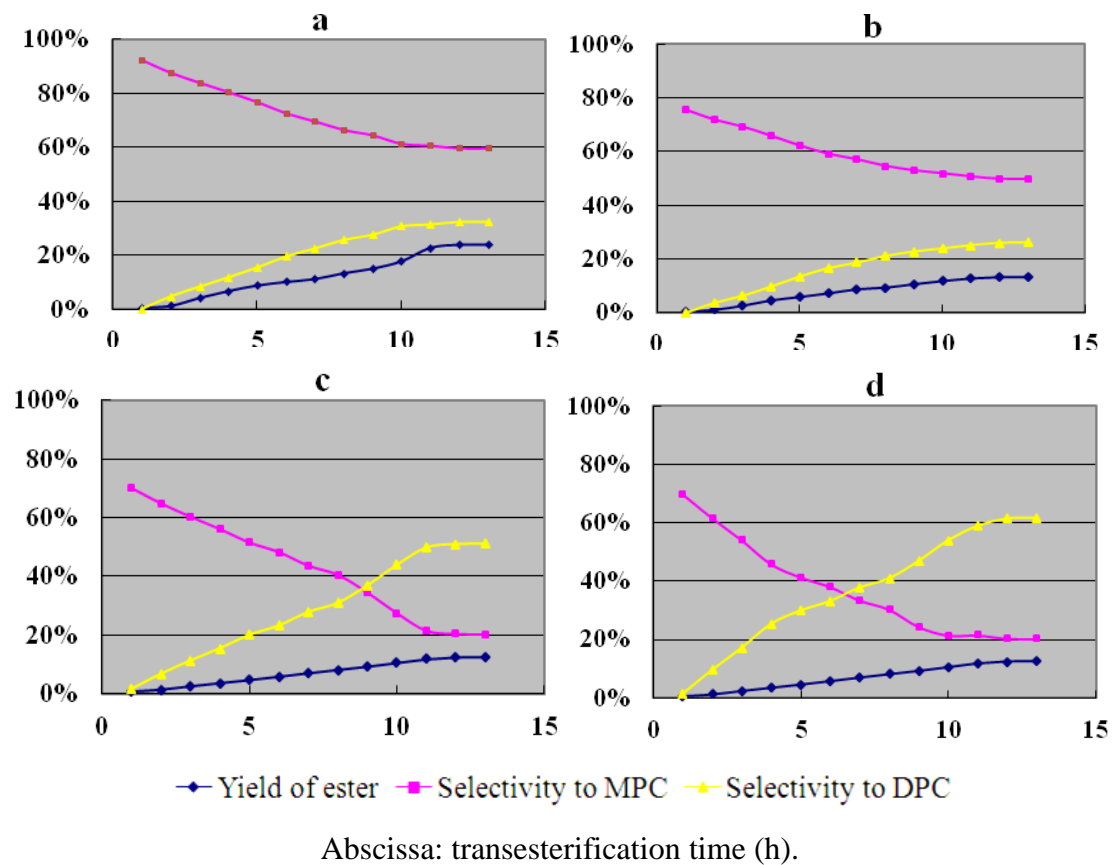


Fig. 5

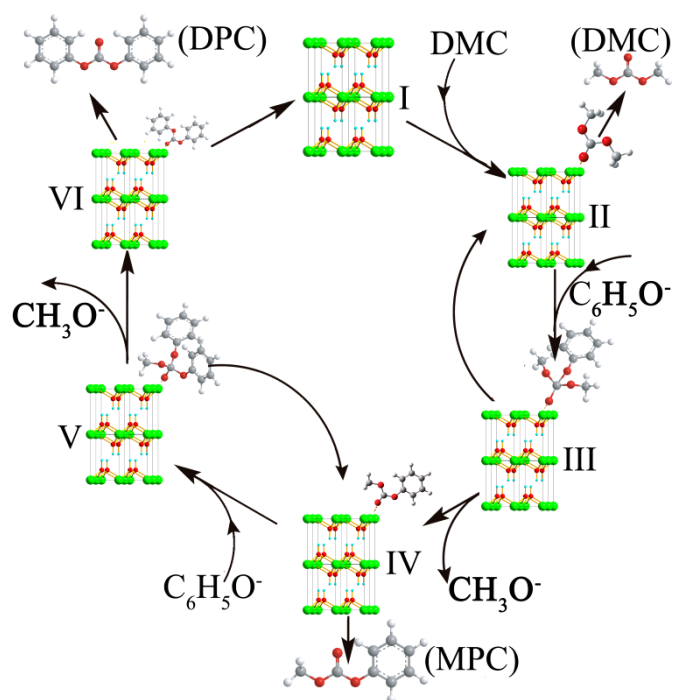


Fig. 6

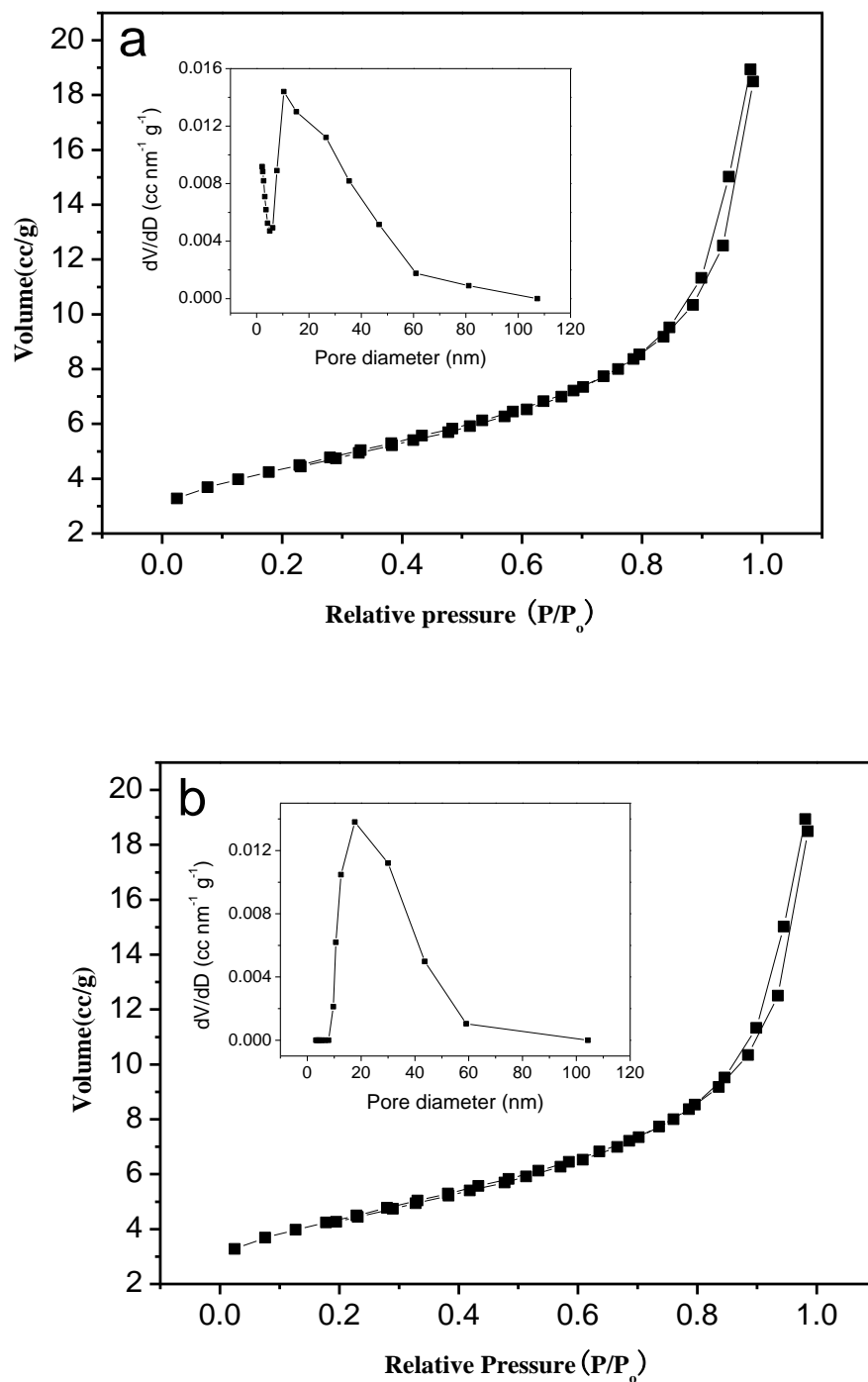
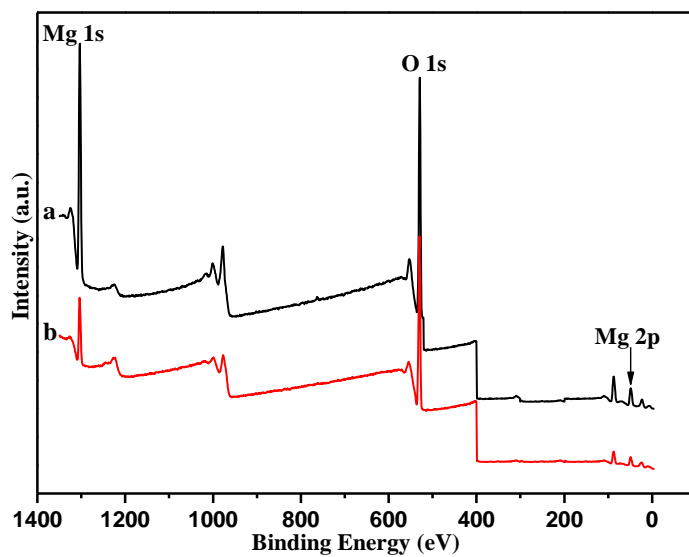


Fig. 7



**Table 1**

<i>T</i> /K	$\Delta_r H_m^\ominus$ KJ mol <sup>-1</sup>	$\Delta_r S_m^\ominus$ J mol <sup>-1</sup> K <sup>-1</sup>	$\Delta_r G_m^\ominus$ KJ mol <sup>-1</sup>	$K_{eq}^\ominus$
298	64.4	- 3.6	65.4	$3.5 \times 10^{-12}$
373	49.6	65.3	25.2	$2.9 \times 10^{-4}$
423	45.9	56.0	22.2	$1.8 \times 10^{-3}$
453	43.0	49.1	20.8	$4.0 \times 10^{-3}$
493	- 45.2	- 146.1	26.8	$1.4 \times 10^{-3}$
523	- 41.2	- 133.9	28.8	$1.3 \times 10^{-3}$

Table 2

$T/K$	$\Delta_r H_m^\ominus$ KJ mol <sup>-1</sup>	$\Delta_r S_m^\ominus$ J mol <sup>-1</sup> K <sup>-1</sup>	$\Delta_r G_m^\ominus$ KJ mol <sup>-1</sup>	$K_{eq}^\ominus$
298	25.9	192.9	-32.6	$5.1 \times 10^5$
373	10.7	151.1	-45.7	$2.5 \times 10^6$
423	13.4	158.2	-53.5	$4.1 \times 10^6$
453	52.5	247.6	-59.7	$7.6 \times 10^6$
493	10.7	154.9	-65.7	$9.1 \times 10^6$
523	14.8	165.6	-71.8	$1.5 \times 10^7$

**Table 3**

Catalyst	Yield of MPC <sup>c</sup> (%)	Yield of DPC <sup>d</sup> (%)	Yield of Anisole(%)	Selectivity to MPC(%)	Selectivity to DPC(%)	Transesterification Selectivity (%)
Mg(OH) <sub>2</sub> <sup>a</sup>	6.1	17.8	1.3	59.7	32.6	92.3
Mg(OH) <sub>2</sub> <sup>b</sup>	4.3	8.9	3.7	49.6	26.1	75.7
AlCl <sub>3</sub>	3.2	15.1	1.1	20.3	51.1	71.4
ZnCl <sub>2</sub>	1.5	11.0	1.2	8.8	61.5	71.3

\* Reaction conditions: molar ratio of phenol-to-DMC 2:1, reaction time:13 h,

temperature:453 K. DPC yield was based on the amount of DMC.

<sup>a</sup> hexagonal Mg(OH)<sub>2</sub> nanoflakes.

<sup>b</sup> irregular Mg(OH)<sub>2</sub> flakes.

<sup>c</sup> MPC: methyl phenyl carbonate. DPC: diphenyl carbonate.

<sup>d</sup> DPC: diphenyl carbonate.

**Table 4**

Numbers of Catalyst Reuse	Yield of MPC <sup>b</sup> (%)	Yield of DPC <sup>c</sup> (%)	Total Yield of Esters (%)	Transesterification Selectivity (%)
1	6.1	17.8	23.9	92.3
2	5.2	17.5	22.7	95.4
3	4.4	14.1	18.5	95.2
4	3.9	13.0	16.9	95.0
5	3.6	12.5	13.1	94.9
6 <sup>d</sup>	5.5	16.2	21.7	91.8

<sup>a</sup> Reaction conditions: molar ratio of phenol-to-DMC 2:1, reaction time:13 h, temperature:453 K.

<sup>b</sup> MPC: methyl phenol carbonate.

<sup>c</sup> DPC: diphenyl carbonate.

<sup>d</sup> Catalyst used fourth and then calcined at 573 K under vacuum.

## Scheme 1

